arXiv:2607.21535v2 [cs.LG] 30 Oct 2026

Windowed-MTP: Removing the Full-Context Draft-KV Tax at Million-Token Context

Alagappan Valliappan
NVIDIA
avalliappan@nvidia.com

Abstract

Speculative decoding accelerates autoregressive generation by having a *draft* propose tokens that a *target* verifies in parallel. Frontier models increasingly ship a built-in Multi-Token-Prediction (MTP) draft head, assumed to be cheap beside verification. **A shipped full-attention MTP head can become disproportionately expensive beside a hybrid target at long context.** The head attends over the full KV cache for each of γ draft forwards per decode step, while only 9–25% of target layers retain full attention, so a single draft layer can issue context reads at a rate comparable to the whole target. On hard, low-acceptance workloads, deep native MTP becomes *net-negative*—slower than no speculation.

We apply a StreamingLLM-style window plus attention sink to the *draft* only (**Windowed-MTP**); target verification remains full-context, so the target distribution is preserved. The intervention is training-free and drop-in. On three models from two hybrid families (Gated DeltaNet and Mamba2) at 1M context on one GPU in SGLang [Zheng et al., 2024], it provides an acceptance-free **1.28–1.44× per-decode-step speedup** over native MTP. The speedup grows with context; at matched acceptance, TPOT improves by the same factor. The window removes most of the draft's working set, and a compact ring buffer converts that reduction into physical capacity: it reclaims the otherwise dead draft pool—a measured 7.7–11.1% of total KV at 1M—making room for one additional concurrent 1M request in the Qwen-35B batch sweep.

1 Introduction

Speculative decoding (SD) [Leviathan et al., 2023, Chen et al., 2023a] reduces autoregressive latency by proposing γ candidate tokens and verifying them in one batched target forward. Recent frontier models bake the draft into the target as a lightweight Multi-Token-Prediction (MTP) head [DeepSeek-AI et al., 2024, Qwen Team, 2026a,b], avoiding a separate draft model.

Standard SD analyses model a draft forward as costing a fixed, small fraction of a target forward [Leviathan et al., 2023]. For a one-layer MTP head that is a fair assumption at short context, but at long context the fraction is neither small nor fixed. Hybrid and linear-attention targets (GDN, Mamba2) reduce verification's KV cost, whereas the MTP heads on the models we study retain full softmax/GQA attention. At γ=6, the single draft layer reads the full KV cache six times per step. The targets we test have only 8–12 full-attention layers, each read once, so the draft does 50–75% as much KV-read work as the entire target. This *long-context draft tax* can erase, and on hard workloads invert, SD's speedup. At the d=7 operating point, native MTP falls *below* the dense baseline on hard 1M tasks (0.86× on Qwen-122B code QA, 0.58× on Nemotron CWE; Table 4).

A draft only needs to be a *good enough guesser*; it need not reread the whole million-token history. We therefore apply a StreamingLLM-style sliding window plus attention sink [Xiao et al., 2024] to the **draft's attention only**, leaving verification at full attention. The draft working set

becomes W + sink tokens (4K is 0.4% of 1M), with no training, extra parameters, or distillation, and a ring buffer converts the smaller working set into physical capacity.

Contributions.

1. We quantify the **long-context draft-attention tax** in built-in MTP heads. At 1M (γ=6), the draft alone takes 61–102% as long as the target's verify pass; with fixed speculative bookkeeping, speculation's overhead is 92–138% of it (Table 2). We give a per-decode-step model that predicts when a deep native draft reaches parity with, or falls below, dense decoding (§3).

2. We retrofit a **training-free window+sink onto the draft attention** (**Windowed-MTP**[1]) of heads that were *trained* at full attention, at serving time and with the verifier unchanged (§4). On three models from two hybrid families it gives a **1.28–1.44× acceptance-free per-decode-step speedup at 1M** (B=1), widening from 1.17–1.27× at 261K, with magnitude tracking the windowable share of draft cost (§6).

3. We **measure how windowing changes acceptance, and why**. We sweep the window size, break acceptance down by draft position, and measure in live runs how often windowing changes the draft's top-1 proposal: it stays the same 86–94% of the time. Acceptance usually changes little (median windowed-to-native ratio 0.96 over 15–16 prompts per task); the largest task-level median loss is 19%. The per-step saving outweighs the loss on every model–task cell we measure (§5).

4. The draft KV pool is a **measured** 7.7–11.1% **of total KV** at 1M; windowing renders all but W+sink of it dead, and a compact **ring buffer converts that into physical capacity** at no quality or speed cost. In the Qwen-35B batch sweep, with each arm at its best feasible memory setting, it fits a sixth concurrent 1M request where native fits five (§6).

2 Background and related work

Speculative decoding and MTP heads. SD [Leviathan et al., 2023, Chen et al., 2023a] pairs a draft with a target verifier. Draft designs range from a separate small model [Leviathan et al., 2023] to self-drafting with extra prediction heads on the target itself [Cai et al., 2024] to feature-level autoregression (EAGLE) [Li et al., 2024a,b]. Frontier models such as DeepSeek-V3 [DeepSeek-AI et al., 2024] and Qwen3.5/3.6 [Qwen Team, 2026a,b] ship a built-in MTP head, which we target here. Acceptance length AL (mean tokens accepted per verify step) governs the speedup; prior work optimizes AL via better draft alignment or tree drafts [Li et al., 2024b]. Our work is orthogonal: we reduce the draft's *cost* at long context without touching the verifier.

Long-context SD. MagicDec [Sadhukhan et al., 2024] observes that at long context and large batch the SD bottleneck shifts to KV loading, and uses a sparse KV cache in a self-speculative decoding setup. We share that diagnosis but focus on the *built-in MTP draft head* of shipping models, and analyze when windowing preserves or trades acceptance. Closest to us, LongSpec [Yang et al., 2026] *trains* a dedicated draft with a constant-size KV cache and hybrid tree attention (dense targets, ≤64K), while SpecExtend [Cha et al., 2026] is training-free but relies on a *separate* draft

[1]Reproduction package (SGLang patch, run/config scripts, seeded inputs): `https://github.com/avalliappan-nvidia/windowed-mtp-b200/tree/master`. The windowed draft attention is merged upstream in SGLang (PR #32673).

model with a cross-model retrieval KV policy, at shorter long-context regimes than the 1M we target. We instead window the *already-shipped* MTP head of hybrid-attention models at 1M, where a cheap verifier *exposes* the draft's $O(S)$ read, inside a production serving framework (continuous batching, paged/radix KV, CUDA-graph capture).

Streaming attention and context extension. StreamingLLM [Xiao et al., 2024] shows that retaining a few initial "sink" tokens plus a recent window preserves fluency under bounded attention; we repurpose this as a *draft-only* approximation. SpecExtend [Cha et al., 2026] argues StreamingLLM-style windowing struggles on needle retrieval, but that is for a *separate* small draft whose only route to a distant needle is its own attention. An MTP head instead conditions on the target's last hidden state, which already carries the target's full-context retrieval, so windowing the draft's own attention removes much less (§5). As in any SD scheme, a missed far token costs at most a rejection, never a wrong answer. Concurrent work [Eldenk et al., 2026] independently reports drafter "attention drift" toward recent tokens (EAGLE-3 and MTP heads) and windows the draft at $\leq$32K as an evaluation tool alongside a training-time post-norm fix; we make windowing a training-free 1M serving technique with draft-KV reclamation. RoPE [Su et al., 2024] with position interpolation [Chen et al., 2023b] and YaRN [Peng et al., 2023] enables the million-token contexts we study; to show the tax and its fix are not RoPE-specific, we also evaluate a Mamba2-hybrid [Gu and Dao, 2023, Dao and Gu, 2024] whose attention uses no position embedding (NoPE).

Drafts windowed at training time. Three recent releases ship MTP drafters whose attention is partly or wholly local. MiMo-V2-Flash [Xiaomi LLM-Core Team et al., 2026] is the most direct: its MTP block uses sliding-window attention with *no* global attention at all, at a 128-token window, and states the reason outright—to cut KV-cache and attention cost. Gemma 4 [Gemma Team et al., 2026] uses a four-layer drafter with three local layers and one global, and Inkling [Thinking Machines Lab, 2026] chains single-layer heads with full or sliding-window attention over a mostly-SWA backbone at 1M. We read these as corroboration rather than competition: they show publicly that a draft need not read the whole context.

The delta is train time versus serving time. These releases establish that a drafter *trained* with local attention works. None addresses whether a head *trained* at full attention tolerates being windowed at inference—the question facing anyone serving an already-published checkpoint, who cannot retrain it. That retrofit is our result, and is why the contribution is aimed at the runtime rather than the model card. Independently of it, none of the three quantifies the tax or gives a cost model predicting where speculation inverts.

Serving systems. We build on paged-KV serving [Kwon et al., 2023] and implement Windowed-MTP in SGLang [Zheng et al., 2024]. The draft's paged block table is reduced to sink plus recent blocks, a graph-safe change requiring no new attention kernel on either the FlashInfer or Triton draft backend. Public serving support now provides this logical sink-plus-recent KV selection for built-in MTP/EAGLE draft decoding. Our evaluated system additionally bounds the *physical* draft-KV allocation: entries excluded from the read set are not merely skipped at attention time, but need not remain resident. We compact them into an $O(n_{\text{sink}}{+}W{+}d)$ ring buffer, freeing HBM for additional concurrency (§6). The compact-ring remap currently uses the Triton draft backend.

3 The long-context draft-attention tax

Cost of one decode step. A speculative decode step runs γ draft forward passes, proposing γ tokens; the target verifies them in one forward and appends one bonus token, so a step commits between 1 and γ+1 tokens, on average the acceptance length AL. We index runs by this cap, $d \equiv \gamma{+}1$ (SGLang's `num_draft_tokens`), and report $d \in \{3, 5, 7\}$, i.e. $\gamma \in \{2, 4, 6\}$ draft forwards. One step takes

$$\text{step} = \underbrace{t_{\text{verify}} + t^{\text{ctx}}_{\text{draft}}}_{c} + \gamma\, t^{\text{fwd}}_{\text{draft}}, \qquad \text{TPOT} = \frac{\text{step}}{\text{AL}}. \tag{1}$$

t_{verify} is the target's verify forward over the d-token block (the bare verify) plus fixed speculative bookkeeping (tree build, sampling). The draft phase $t_{\text{draft}} = t^{\text{ctx}}_{\text{draft}} + \gamma\, t^{\text{fwd}}_{\text{draft}}$ has two terms: $t^{\text{ctx}}_{\text{draft}}$, a once-per-step build of the draft's KV index over the whole context, and $t^{\text{fwd}}_{\text{draft}}$, one draft forward, which rereads the draft's KV. Both grow as $\mathcal{O}(S)$, so the native draft pays for the full context in both terms. To first order, none of the terms depends on how many tokens a step accepts; their fitted values drift only modestly across workloads (App. C). Windowing targets the two draft terms.[2]

Break-even acceptance length. Dense decoding commits one token per step, so its TPOT is its step time. Speculation at depth d therefore beats dense exactly when its AL exceeds the *break-even* AL, the number of dense steps that fit in one native speculative step:

$$\text{AL}(d) \;>\; \text{AL}_{\text{break-even}}(d) = \frac{\text{step}^{\text{native}}(d)}{\text{step}^{\text{dense}}}. \tag{2}$$

The break-even AL uses only acceptance-free step times, so it is known before any request arrives. At d=7 and 1M it is 2.7–2.9 for Qwen-35B, 3.6–3.9 for Qwen-122B and 2.9–3.0 for Nemotron; the ranges come from dense TPOT varying across tasks. The engine already logs the accepted length of every step, so a server can compare its running AL with the break-even AL and lower d, or turn speculation off, when it falls below.

Calibrating the model. The break-even test needs only two step times at the deployed depth, from one dense and one native run at the target context length on any input. Step time is the time per decode iteration, AL × TPOT, which any engine that reports acceptance and throughput provides (in SGLang, accept_len/throughput); AL cancels, so it does not depend on acceptance. Measuring native at two or more depths and fitting the line $\text{step} = c + \gamma\, t^{\text{fwd}}_{\text{draft}}$ adds two things: the break-even AL at unmeasured depths, so a server can pick d rather than only switch speculation off, and the split of the tax into the intercept c and the per-forward slope $t^{\text{fwd}}_{\text{draft}}$ (below). Two refinements apply. (i) On Qwen-122B and Nemotron the verify cost jumps once, by ≈6 ms, at d=5, where its attention crosses a kernel tile boundary; depths on either side need their own fit (we fit d=5–8; App. B). (ii) Every term grows with context, so the constants are calibrated per context length and batch size. Calibrated on `niah_multiquery_enum` alone, the break-even AL flags all six cells of Table 4 where native is slower than dense, plus three near-ties where native is at most 7% ahead. Across d=5–8 on the other inputs, the fitted line flags all 20 losing cells (App. C).

Measuring the tax. Table 1 gives the fitted constants and the measured step at d=7. Windowing saves 7.3–8.1 ms per step, nearly all in the draft phase: t_{verify} is unchanged on the Qwen models and drops 1.2 ms on Nemotron (Table 2). Both draft terms shrink. The intercept c falls by 5.1–6.1 ms,

[2]The target verify also grows with S, but windowing leaves the target path untouched, so it is not a lever here.

almost all of it the draft's index build, which windowing nearly eliminates. This part depends on the implementation and a leaner index kernel would shrink it, but windowing stays 1.07–1.16× faster per step even if native's index build were free (App. B). The slope $t_{\text{draft}}^{\text{fwd}}$ falls 22–40%, worth 1.9–2.9 ms at γ=6. This part comes from reading a bounded window instead of the whole context, so it holds on any backend, and it matters more as hybrid targets make verification cheaper. Before windowing, the draft and bookkeeping together cost 92–138% of the bare verify pass, so speculation roughly doubles the step; windowing cuts this to 45–72%. The per-step speedup is 1.28× (Nemotron) to 1.44× (Qwen-35B), and the end-to-end speedup over native is this times the change in acceptance:

$$\frac{\text{TPOT}^{\text{native}}}{\text{TPOT}^{\text{win}}} = \frac{\text{step}^{\text{native}}}{\text{step}^{\text{win}}} \cdot \frac{\text{AL}^{\text{win}}}{\text{AL}^{\text{native}}}. \tag{3}$$

The first factor is fixed for a model and context length; the second depends on the workload (§5).

Table 1: Per-step decode cost at 1M, B=1 (bf16 KV, single B200), native→windowed, on `niah_multiquery_enum` (step is within 3% on most inputs and up to 9% shorter on aggregation inputs; App. C). c and $t_{\text{draft}}^{\text{fwd}}$ are the line of Eq. 1 fitted over d=5–8 ($R^2 \geq 0.97$; Qwen-122B over d=5–7, since d=8 does not fit at 1M). Step is measured at d=7 (γ=6) without profiling and agrees with $c+6\,t_{\text{draft}}^{\text{fwd}}$ within 0.3 ms. Speedup is $\text{step}^{\text{nat}}/\text{step}^{\text{win}}$, the gain at matched acceptance.

model	c (ms)	$t_{\text{draft}}^{\text{fwd}}$ (ms)	step (ms)	speedup
Qwen-35B	19.3→14.2	1.19→0.71	26.4→18.3	**1.44**×
Qwen-122B	27.6→21.5	1.16→0.85	34.5→26.5	**1.30**×
Nemotron	24.6→19.1	1.45→1.13	33.1→25.8	**1.28**×

Table 2: Per-iteration wall-clock phases from the nsys trace (d=7, 1M, B=1; mean over 18 steady iterations, native→windowed). $t_{\text{verify}}^{\text{base}}$: the target's verify forward over the d-token block; $t_{\text{verify}}^{\text{ovh}}$: speculative bookkeeping (tree build, sampling); together they form t_{verify}. Profiling adds 2–5 ms per iteration relative to Table 1.

model	$t_{\text{verify}}^{\text{base}}$	$t_{\text{verify}}^{\text{ovh}}$	t_{draft}	Iteration
	(ms/iter, native→windowed)			
q35	12.5→12.4	4.6→4.6	**12.7→4.3**	29.7→21.3
q122	19.5→19.6	4.3→4.2	**13.6→7.3**	37.4→31.1
nem	19.0→19.0	5.8→4.6	**11.6→4.0**	36.5→27.6

Why native speculation collapses at long context. On hard tasks AL levels off well below d, while every extra draft forward still adds $t_{\text{draft}}^{\text{fwd}}$, which at 1M includes a full-context read. The numerator of Eq. 1 keeps rising with d and the denominator does not, so TPOT climbs back past dense, which pays for neither the draft nor the bookkeeping. On the large models the verify tile jump at d=5 adds a further ≈6 ms that deeper drafts pay without any acceptance gain. The tax is specific to long context, though not because the draft outgrows the target: both read $\mathcal{O}(S)$ of KV, so the draft's share of the work is the same at any length. What changes is whether those reads cost time. A draft layer's KV is ≈1–2 KB/token, so at 8–32K its 8–64 MB can fit in the B200's 126 MB L2, potentially reducing the HBM traffic of the γ re-reads. At 1M the 1–2 GB draft KV far exceeds L2, so each draft forward must stream it from HBM. More on-chip capacity or bandwidth moves the context length at which the tax appears; it does not remove it.

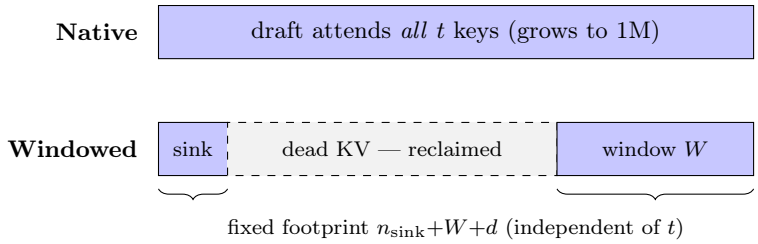


Figure 1: Draft attention before/after windowing. The *native* MTP draft attends the full, growing key set, so its per-draft-step cost and KV footprint scale with context t. *Windowed-MTP* restricts the draft to n_{sink} sink tokens plus the most recent W keys; the intervening keys are never read and are reclaimed by storing the draft KV in a compact $n_{\text{sink}}{+}W{+}d$ ring buffer.

4 Method: Windowed-MTP

Mechanism. At each draft step, the draft attends only to the first n_{sink} tokens (the attention sink) and the most recent W tokens, instead of the whole context (Fig. 1). Each cached key already carries its position, so the draft sees the same scores for these tokens as before; it simply skips the rest. The target's verify pass is unchanged and still attends to the full context. The method is training-free: the engine only changes which cached entries it hands to the draft (implementation in App. A).

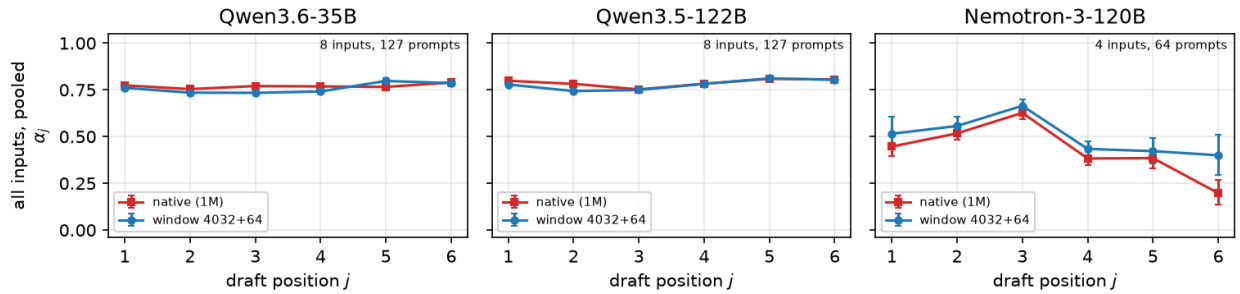


Figure 2: Per-position conditional acceptance α_j (d=7, γ=6, 1M), native (full-1M) vs. windowed (4032+64), for the three models (columns), pooled over every prompt of every input in Table 4 (Qwen: 8 inputs, 127 prompts; Nemotron: 4 inputs, 64 prompts). Error bars: 95% cluster-bootstrap intervals over prompts, stratified by input. Same runs as Table 4.

Why this preserves the target distribution. Let the full-context target induce $p(\cdot \mid x_{<t})$ and the draft induce q. Under speculative sampling, a proposal is accepted under the standard p/q rule; after a rejection, the replacement is sampled from the residual distribution proportional to $[p-q]^+$. This procedure returns exactly p, regardless of q. Under greedy decoding, the target accepts the matching proposal prefix and appends its own token at the first mismatch. Replacing a full-attention q with q^{win} therefore changes only proposals and acceptance; in exact arithmetic, greedy output is bit-exact.

In practice, `bf16` SD is not bit-exact against dense. Verifying d tokens in one batched forward reorders floating-point reductions, so occasional argmax near-ties flip and compound. This is a property of the verification batch, not of windowing: it affects native and windowed drafts alike, just as it separates two native depths. The relevant comparison is therefore windowed versus native, not

either versus dense. Our patch does not modify the target verify path, so the guarantee rests on the standard verifier; we have not yet quantified the bf16 divergence rates between arms.

Memory. Capping the draft's KV pool to a $W + n_{\text{sink}}$ ring buffer frees the remainder of what would otherwise be a full-length draft cache—an architecturally-fixed **7.7–11.1% of total KV** across our three models (§6)—and that budget converts directly into serving headroom. At 1M on a single B200, with each arm at its best feasible memory setting, the ring buffer lets Qwen-35B (d=7) seat B_{eff}=6 concurrent requests at a 6.28M-token KV pool where native MTP seats five (Fig. 4; App. A). The ring keeps the sink fixed and reuses the recent slots circularly; App. A explains why it never reads an overwritten entry and needs no rollback after a rejection.

5 How windowing changes acceptance

Eq. 3 shows the speedup has two factors: a cost factor ($\text{step}^{\text{native}}/\text{step}^{\text{win}} > 1$, always favorable) and an acceptance factor $\text{AL}^{\text{win}}/\text{AL}^{\text{native}}$. A naive expectation is that windowing can only *lose* acceptance (the draft sees less). In practice the change is usually small and goes both ways: across the 20 cells the median per-prompt ratio is 0.96 and is above 1 on six (Table 16), but it falls by 16–19% (task-level medians) on Qwen-35B NIAH-mv and VT. This section explains why the change is usually small, and why the cheaper step still outweighs the larger losses.

Window size. Fixing d=7 (γ=6 draft forwards) and sweeping the window W on `niah_multiquery_enum` at 1M (16 prompts, Table 3), every window from 1K to 8K beats native on every model: 1.29–1.35× on Qwen-35B, 1.14–1.17× on Qwen-122B and 1.27–1.31× on Nemotron (median per-prompt speedup), with every 95% bootstrap interval above 1.10. Acceptance is just as flat (median per-prompt ratio to native 0.93–0.96, 0.88–0.90 and 0.99–1.02). The needles sit outside both the 4K and 8K windows, so a larger window adds only distant context and does not raise acceptance; it only re-adds the draft's $\mathcal{O}(S)$ tax. The gain therefore does not hinge on tuning W. On Qwen-35B the default ∼4K window keeps 96% of native acceptance and cuts median per-token latency from 5.86 to 4.17 ms.

Table 3: Window and sink ablation (d=7, 1M, B=1, `niah_multiquery_enum`, 16 prompts): median AL and median per-prompt TPOT speedup over the native full-context draft. Window columns use sink 64; sink columns use W=4032. The operating point (W=4032, sink 64) is bold.

			window W (sink 64)				sink (W=4032)		
model		native	960	1984	**4032**	8128	0	32	128
q35	AL	4.45	4.45	4.53	**4.43**	4.21	4.36	4.59	4.23
	speedup	1.00×	1.32×	1.35×	**1.34**×	1.29×	1.34×	1.39×	1.32×
q122	AL	4.76	4.30	4.25	**4.32**	4.45	4.18	4.28	4.32
	speedup	1.00×	1.15×	1.14×	**1.16**×	1.17×	1.13×	1.16×	1.17×
nem	AL	3.63	3.70	3.70	**3.68**	3.49	3.17	3.60	3.80
	speedup	1.00×	1.30×	1.31×	**1.27**×	1.27×	1.16×	1.27×	1.28×

Sink size. The sink costs 64 of the draft's 4,096 slots, and removing it lowers acceptance on all three models (Table 3). The loss is largest on Nemotron: the median per-prompt ratio to sink 64 is 0.87, which cuts its speedup over native from 1.27× to 1.16×. Qwen-122B follows (0.95, 1.16→1.13×), then Qwen-35B (0.99); with 16 prompts no interval excludes 1. A 32-token sink

recovers the loss on all three models, and from 32 to 128 the median ratio to sink 64 stays within 0.02, so the sink size needs no tuning either.

Across inputs. Across the full d=7 sweep (Table 4) the acceptance factor varies in sign with input and model, but in no model–task cell does it cancel the per-step saving: the median nat/win is $\geq$1.14$\times$ on every cell. A direct in-run probe (Table 11) shows why the change is usually small: windowing leaves the draft's top-1 proposal unchanged 86–94% of the time.

Per-position decomposition. We read SGLang's per-request acceptance histogram $H[n]$ (number of verify steps that accepted exactly n draft tokens) and derive the *conditional* acceptance rate at draft position j,

$$\begin{aligned} \alpha_j &= \Pr[\text{accept } j \mid \text{reached } j] = \frac{\sum_{n \geq j} H[n]}{\sum_{n \geq j-1} H[n]}, \\ \mathrm{AL} &= 1 + \sum_{j \geq 1} \prod_{k \leq j} \alpha_k. \end{aligned} \tag{4}$$

Figure 2 shows α_j (d=7, γ=6, 1M) for native vs. windowed drafts, pooled over every prompt of every input in Table 4. The windowed profile *tracks* the native one position by position. On both Qwen models the two differ by at most 0.04 at any position (largest: Qwen-122B at j=2, 0.78→0.74), and α_1 (local prediction) by at most 0.02. With 127 prompts per model some of these gaps are statistically resolvable, but none is large. On Nemotron the windowed draft accepts more at every position. Neither profile collapses at the deep, compounding positions. Single inputs spread more widely. The largest per-input drop is Qwen-35B NIAH-mv at j=2 ($-$0.18), the cell whose median AL falls most, and Qwen-122B, the strongest drafter, loses 11–13% on multi-query and multi-value retrieval (median ratios 0.89 and 0.87, Table 16), where far context is *informative* rather than dilutive. Across all inputs (Table 4) the change is usually small, but not always: Qwen-35B's median loss is 19% on NIAH-mv and 16% on VT, giving end-to-end gains of 1.15$\times$ and 1.21$\times$.

Pooled over inputs, the acceptance difference arises mainly past the first draft position: α_1 barely moves on the Qwen models, so a shallow draft is nearly windowing-invariant and the gap emerges only as d grows (App. E). The cost factor is favorable at every depth; acceptance is a second-order term on top.

Why windowing rarely changes the draft's choice. All three drafts sit on recurrent-hybrid models (Gated-DeltaNet for Qwen, Mamba2 for Nemotron), whose recurrent layers already carry long-range information, so the draft's reread of distant context mostly repeats what it already has. This holds even for Nemotron, whose NoPE attention puts ≈84% of its softmax mass outside the window, yet whose top-1 proposal is preserved 86% of the time. On the RoPE Qwen drafts, the ≈20–25% of mass beyond the window is diffuse rather than peaked on a few informative keys (App. D, Table 12). The argument is specific to hybrid targets; a draft on a dense-attention model may lean more on distant context. We treat it as interpretation, not proof.

6 Experiments

Setup. Unless noted, we use one NVIDIA B200 (TP1), bf16 KV, and SGLang with its built-in MTP speculative decoding and CUDA graphs; Fig. 5 instead uses two B200s at TP2. The models are

Qwen3.6-35B-A3B and Qwen3.5-122B-A10B (GDN-MoE, MoE-FFN MTP), and Nemotron-3-Super-120B-A12B (Mamba2-hybrid, eight GQA full-attention layers, MoE-FFN MTP, NoPE); checkpoints are in App. A. Windowed-MTP uses W=4032, n_{sink}=64.

At a fixed 1.04M-token input, we evaluate RULER [Hsieh et al., 2024] retrieval and aggregation tasks, LongBench-v2 [Bai et al., 2024] code-reasoning QA, and BABILong [Kuratov et al., 2024] multi-fact QA. We report acceptance, time per output token (TPOT), and speedup over native MTP and dense decoding. Unless noted, all arms decode greedily (temperature 0) with a repetition penalty of 1.15, which prevents enumeration loops from artificially inflating acceptance. Each task uses QA mode, stopping at EOS or 512 new tokens. Thus every timed decode step attends to an effectively fixed ∼1M-token cache—the long-prompt, short-completion regime. The same draft-cost mechanism applies when a short prompt reaches that length through generation instead.

No input is tiled or repeated to reach length, all inputs come from seeded generators that reproduce byte-for-byte, and positional validity at 1M is handled at the model level (YaRN for Qwen, native NoPE for Nemotron), applied identically to the dense baseline and every speculative variant (App. A). Table 4 reports multi-prompt results: 16 independently generated prompts per task (15 for Code-QA); each model–task cell reports the median over them. The cost model, the depth ablation and the batch sweeps use one reference prompt per task (the first of the 16) unless stated otherwise; the sampling and online runs are described where they appear.

Results across all inputs. Table 4 reports every task at d=7. Windowed-MTP is faster than native MTP on every model–task cell, by a median 1.14–1.56×, and 1.03–2.54× faster than dense decoding. Native MTP, in contrast, is slower than dense on six cells and ties it on a seventh. Acceptance changes little: the median windowed-to-native AL ratio is 0.96, 16 of the 20 cells are within ±15% (unrounded), and windowing raises AL on six (Table 16). Eq. 3 splits each prompt's speedup into a per-step factor and an acceptance factor. The per-step factor is nearly constant across prompts (cell medians 1.40–1.44× on Qwen-35B, 1.28–1.31× on Qwen-122B and 1.26–1.27× on Nemotron), so variation across prompts and tasks tracks acceptance, and the smallest gains come where acceptance drops most: Qwen-35B NIAH-mv (AL ratio 0.81, 1.15×) and Qwen-122B NIAH-mv and BABILong (0.87 and 0.90, both 1.14×). Even there, the cheaper step outweighs the lost acceptance (per-prompt spread in App. G). The per-step gain is smallest on Nemotron, whose windowable share of draft cost is smallest (§7).

The per-step cost saving grows with context. The windowing wedge widens as context grows because windowing removes the *draft's* $\mathcal{O}(S)$ context cost: as S grows the native draft's full-context scan adds increasing cost, while the windowed draft's attention working set stays fixed (4K is 1.6% of 261K but 0.4% of 1M); target verification remains context-dependent under both. Sweeping the true-1M input (`niah_multiquery_enum`, d=7, matched acceptance, Table 1) from 261K to 1M (Fig. 3), the matched-acceptance speedup rises for all three models (Qwen-35B 1.27→1.43×, Qwen-122B 1.24→1.30×, Nemotron 1.17→1.26×). The absolute per-step saving Δ roughly doubles in each case (3.4→7.9, 3.5→7.8, 3.2→6.8 ms).

Best-depth baseline. A practitioner tunes draft depth per model and keeps the fastest, so the fair comparison is native at *its* best depth vs. windowed at *its* best depth. Table 5 sweeps every depth from d=2 to 8 on the multi-query retrieval input at 1M (Qwen-122B stops at d=7, as d=8 does not fit its KV pool). **At each method's best depth, Windowed-MTP is faster than native on all three models** (1.18–1.41×), and it is also faster at every individual depth. The best depths differ. Native's TPOT is non-monotonic in d: each extra draft forward pays the full-context

Table 4: All inputs at 1M, d=7 (γ=6), B=1, greedy (temperature 0). TPOT in ms; spd is speedup over dense (no speculation); nat/win is native TPOT over windowed TPOT (speedup over native). All arms run the same 16 prompts per task (15 for Code-QA); AL and TPOT are medians over prompts, and spd and nat/win are medians of per-prompt ratios (95% intervals in App. G). Nemotron is shown on its four long-decode tasks; on NIAH-s, VT, Code-QA and BABILong it answers in 4–12 tokens, too briefly to time.

		Dense	native MTP (d=7)			Windowed-MTP (d=7)			nat/win
Model	Input	TPOT	AL	TPOT	spd	AL	TPOT	spd	(TPOT)
Qwen3.6-35B	NIAH-s	9.84	5.07	5.19	1.88×	4.72	**3.90**	2.54×	**1.35**×
	NIAH-mv	9.84	5.42	4.80	2.05×	4.39	**4.24**	2.32×	**1.15**×
	NIAH-mq	9.79	4.45	5.86	1.67×	4.43	**4.17**	2.35×	**1.34**×
	VT	9.72	4.18	6.36	1.53×	3.63	**5.10**	1.90×	**1.21**×
	CWE	9.21	2.74	8.83	1.05×	2.81	**6.15**	1.51×	**1.45**×
	FWE	9.25	2.85	8.68	1.07×	3.02	**5.73**	1.61×	**1.56**×
	Code-QA	9.96	3.30	8.05	1.24×	3.14	**5.98**	1.67×	**1.37**×
	BABILong	9.65	3.07	8.38	1.17×	2.78	**6.54**	1.48×	**1.28**×
Qwen3.5-122B	NIAH-s	9.54	4.04	8.62	1.11×	3.75	**7.17**	1.33×	**1.21**×
	NIAH-mv	9.54	4.81	7.16	1.33×	4.34	**6.07**	1.57×	**1.14**×
	NIAH-mq	9.56	4.76	7.20	1.33×	4.32	**6.04**	1.58×	**1.16**×
	VT	9.60	3.82	9.15	1.05×	3.67	**7.30**	1.31×	**1.25**×
	CWE	8.86	3.28	9.61	0.92×	3.27	**7.47**	1.19×	**1.27**×
	FWE	8.77	3.45	9.17	0.96×	3.44	**7.12**	1.24×	**1.34**×
	Code-QA	9.57	3.16	11.07	0.86×	3.32	**8.01**	1.19×	**1.31**×
	BABILong	9.32	3.64	9.33	1.00×	3.08	**8.54**	1.10×	**1.14**×
Nemotron-3-120B	NIAH-mv	11.35	2.86	11.66	0.97×	3.02	**8.70**	1.30×	**1.26**×
	NIAH-mq	11.39	3.63	9.09	1.25×	3.68	**6.97**	1.63×	**1.27**×
	CWE	10.90	1.64	18.68	0.58×	2.47	**9.83**	1.11×	**1.47**×
	FWE	10.92	1.64	18.51	0.59×	2.30	**10.76**	1.03×	**1.53**×

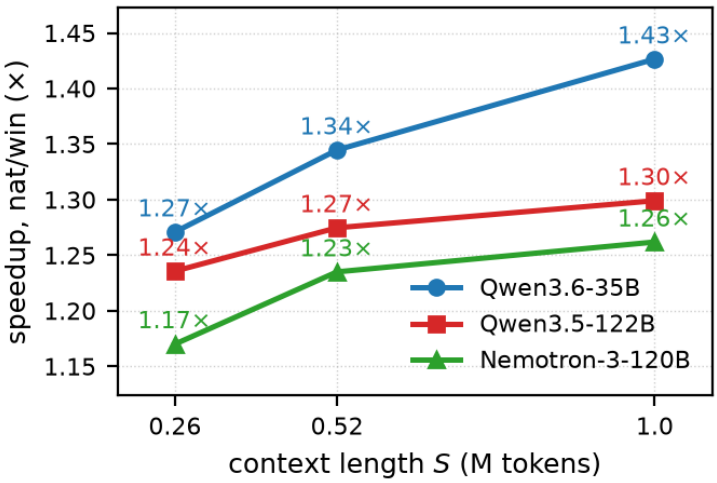


Figure 3: The windowing wedge *widens with context*. Matched-acceptance speedup $\text{step}^{\text{nat}}/\text{step}^{\text{win}}$ (T_{iter}=AL · TPOT, so acceptance cancels) vs. context length S, at d=7, B=1, bf16, on `niah_multiquery_enum`. The 1M endpoints match Table 1 within run-to-run noise ($\leq$0.03×).

Table 5: Best-depth baseline (1M, B=1, `niah_multiquery_enum`): native vs. windowed, each at its own min-TPOT depth over d=2–8 (Qwen-122B: $d\leq$7, as d=8 exceeds the KV pool for both arms). TPOT in ms, best d in parens; dense TPOT for reference. Single run per depth.

model	dense	native (d)	windowed (d)	nat/win
Qwen-35B	9.90	5.47 (6)	3.89 (7)	**1.41**×
Qwen-122B	9.56	6.09 (7)	5.15 (4)	**1.18**×
Nemotron	11.27	7.42 (4)	5.34 (4)	**1.39**×

read, and the large models also pay the verify jump at d=5, so Nemotron's native optimum is d=4. The windowed draft is cheap, so its optimum is set by acceptance instead: it sits deeper than native on Qwen-35B (d=7 vs. 6) and shallower on Qwen-122B (d=4 vs. 7), where the cheaper step more than pays for the tokens it gives up.

Sampling at temperature 1. Our main runs are greedy. To check that the gain carries over to sampling, we rerun Qwen-35B at 1M and d=7 with temperature 1 and the model's released default sampling settings (top-k 20, top-p 0.95, from its `generation_config`), on every prompt of three inputs, averaging three seeds per prompt (Table 6). Sampling lowers native acceptance most on Code-QA (median 3.30→2.77, greedy vs. sampled), while the windowed-to-native AL ratio stays near 1 (0.96–1.07). The per-step speedup is 1.39–1.44× on every seed, matching the greedy 1.44× (Table 1), so windowing is 1.39–1.48× faster than native. On CWE and Code-QA, native is no faster than dense (0.95× and 1.01×, slower on 15 of 16 and 7 of 15 prompts), and windowing brings speculation back above it (1.40× and 1.36×).

Memory. From SGLang's KV-pool allocation logs at 1M, the draft (MTP) KV pool is a **measured 7.7–11.1%** of total KV (7.7/9.1/11.1% for Qwen-122B/Qwen-35B/Nemotron) — matching the architectural $1/(F{+}1)$ share (F full-attention layers =12/10/8 of 48/40/88). Both pools are sized up front to the startup KV budget, so this share is a property of the architecture and that budget

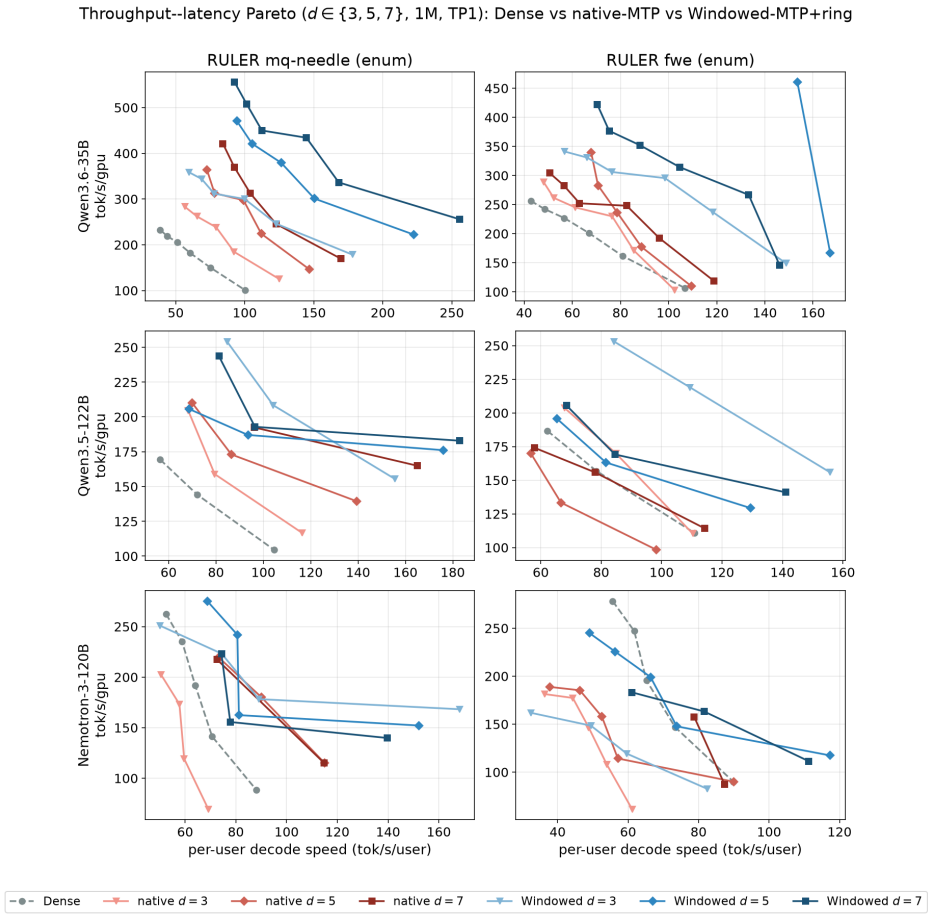


Figure 4: Throughput–latency Pareto at 1M (B sweep over $d \in \{3, 5, 7\}$; single B200, TP1). Rows: Qwen3.6-35B, Qwen3.5-122B, Nemotron-3-120B; columns: `niah_multiquery_enum` and `fwe` (up-and-right is better). Windowed-MTP+ring (blue) holds the frontier over native MTP (red) and Dense (grey) in five of six panels, the exception being Nemotron+FWE (see text), and also fits more resident 1M requests (one more on 35B at each arm's best feasible memory setting).

Table 6: Temperature-1 sampling (top-k 20, top-p 0.95), Qwen-35B, 1M, d=7, B=1; medians over 16 prompts (15 for Code-QA) of per-prompt means over seeds 0–2. TPOT in ms (dense/native/windowed); nat/win is the median per-prompt native over windowed TPOT.

input	AL^{nat}	AL^{win}	TPOT (d/n/w)	nat/win
NIAH-mq	4.57	4.36	9.94/5.89/4.33	**1.39**×
CWE	2.53	2.68	9.35/9.84/6.66	**1.48**×
Code-QA	2.77	2.59	10.07/9.94/7.38	**1.43**×

rather than of any request: invariant to GPU size and KV precision, with the absolute GB scaling linearly (App. A). Windowing reads only $\min(\text{seq}, W{+}n_{\text{sink}})$ base tokens per draft step (structurally guaranteed by the draft-KV index builder), so at 1M ($W{+}n_{\text{sink}}$=4096, ≈0.4% of a 1.04M-token request) > 99% **of the draft pool is dead and reclaimable**. Every Windowed-MTP result here runs the ring ($n_{\text{sink}}{+}W{+}d$ slots per request, confirmed in the same logs). Its payoff is the batch headroom in Fig. 4: the windowed arm seats one more concurrent 1M request, while native's full-length draft pool crowds the target KV and runs out of KV capacity a batch earlier. This holds at each arm's best feasible memory fraction; with windowing given less memory than native (0.90 vs. 0.92), both seat five (App. A).

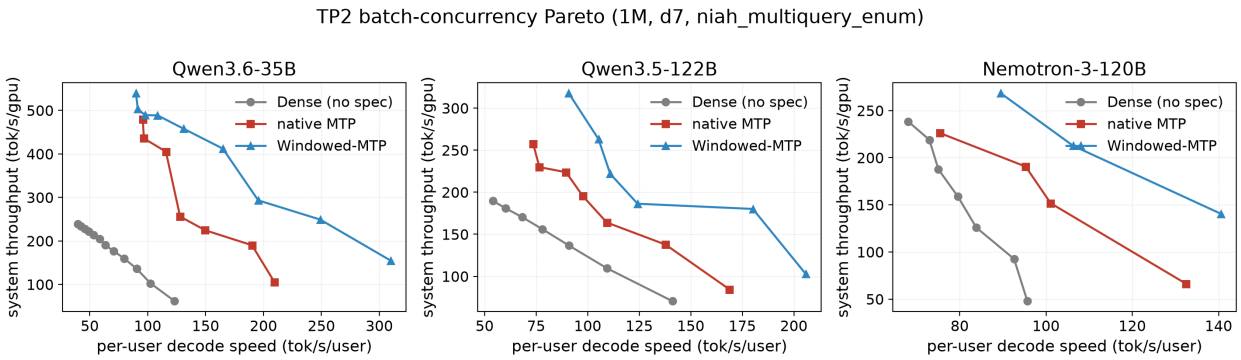


Figure 5: TP2 batch-concurrency Pareto *frontier* (2×B200, 1M, d=7, `niah_multiquery_enum`): per-user decode speed (x) vs. per-physical-GPU throughput (y), sweeping batch B (non-dominated points only). Windowed-MTP (blue) vs. native MTP (red) vs. Dense (grey).

Throughput–latency Pareto. Figure 4 sweeps batch size B at 1M across all three models (rows) and both workloads (columns) on a single B200, over $d \in \{3, 5, 7\}$. Taking Qwen-35B (top row), Windowed-MTP *Pareto-dominates* both Dense and native MTP on both axes at every batch: at B=1 it delivers 2.5× the per-user decode speed of Dense (255.6 vs. 100.4 tok/s/user), and its peak system throughput (556 tok/s/GPU at B=6) is 2.4× Dense's and 1.3× native's. Dominance holds in five of six panels; the exception is Nemotron+FWE, our lowest-acceptance workload, where the frontier splits—windowing wins the latency end but Dense wins peak throughput at high batch, the expected boundary where low acceptance makes speculation unprofitable once the batch is compute-bound.

Tensor-parallel scaling and batch concurrency (TP2). TP2's *primary* purpose here is *capacity*: two B200s hold more concurrent 1M requests than one. We sweep B at TP2 (2×B200, 1M, d=7, `niah_multiquery_enum`) with the radix cache disabled (as for every batch sweep, so

Table 7: H100-80GB replication: Qwen-35B *FP8* (public checkpoint), 1M, B=1, d=7, `bf16` KV, `niah_multiquery_enum`. Windowed-MTP is faster than Dense and native.

method	AL	TPOT (ms)	speedup
Dense	1.00	12.26	1.00×
native	4.34	7.48	1.64×
windowed	4.53	5.05	**2.43**×

each seated request carries a full, independent 1M KV), from B=1 to the largest batch seating a full 1M KV per request (B=12 for Qwen-35B, B=7 otherwise). **Windowed-MTP's frontier Pareto-dominates both Dense and native MTP for all three models** (Fig. 5): at equal batch the cheaper step raises the throughput ceiling 1.13–1.23× above native and 1.1–2.3× above Dense. Points use measured TPOT, which includes acceptance. We do not compare AL across TP degree, as it is not bit-stable there (head splitting reorders the `bf16` reductions, §4). Nemotron's frontier varies more run-to-run but stays windowed-dominated.

Online serving under continuous arrivals. Every result so far fixes the batch, so we also test under a real scheduler: Qwen-35B at TP2, Poisson arrivals at an offered rate of λ requests/s over mixed 131K–1.04M contexts, the prefix cache on, and 4096-token generations, with all three arms replaying the identical trace at a matched memory fraction (App. F). At $\lambda \in \{0.02, 0.05\}$, Windowed-MTP's paired median speedup is 1.15–1.21× over native and 2.0–2.2× over dense (Table 14), and it meets a 25 ms p95-TPOT target at 0.05 req/s, where dense and native meet it only at 0.02 (Table 15). The gain needs long generations, and it does not raise peak throughput: from λ=0.075 up, all arms plateau near 0.06 req/s, because at 1M the server is bound by prefill, which windowing does not touch (App. F).

Cross-hardware generality (H100). The win is not specific to Blackwell memory bandwidth. Reproducing the single-GPU result on one NVIDIA H100-80GB with the *public* FP8 checkpoint (`RedHatAI/Qwen3.6-35B-A3B-FP8`; B=1, 1M, d=7, `bf16` KV, same headline input), Windowed-MTP is again faster than Dense (2.43×) and native (1.48×) and keeps acceptance (4.34→4.53; Table 7).

The backend is not the confound. Native runs on FlashInfer, but we built the ring on Triton because its kernels are simpler to modify for the slot remap. Triton is if anything a *handicap*: on Qwen-35B CWE at d=5, its draft-extend kernel makes native's TPOT ∼6× worse than on FlashInfer (8.13 → 50.59 ms), and its cost grows with accept length. Even so, windowed-on-Triton beats native-on-FlashInfer (5.37 ms). A FlashInfer implementation of the ring remains unmeasured (App. E).

7 Discussion and limitations

Choice of baseline. We compare against the *native full-context MTP* head the target already ships, with its window disabled and weights, verifier and tree shape fixed. Acceptance-optimizing drafts (EAGLE-style trees [Li et al., 2024b], EAGLE-3 [Li et al., 2025], DeepSeek's speculative stack [DeepSeek-AI, 2026]) are complementary: comparing against them would conflate draft training quality with attention cost, and an EAGLE-3 head attends over the full KV cache, so it pays the

same $\mathcal{O}(S)$ tax and the same window applies. Block-diffusion drafters such as DFlash [Chen et al., 2026] keep full-context KV in each draft layer too; measuring windowing on them is future work.

Why not dynamic KV selection? A dynamic selector (per-step top-k as in Quest [Tang et al., 2024], or SpecExtend's cross-model retrieval [Cha et al., 2026]) must keep the *full* KV resident to select from, forfeiting the draft-pool reclamation that is a core benefit here, and its scoring and irregular gather add compute to the very forward we are cheapening—while a static sink+window already keeps acceptance close to native on most inputs (§5).

When to window, and how to pick W. Windowing pays off when the draft's per-step KV cache read is a non-trivial share of the draft forward, i.e. at long context. When $S \lesssim W$ the window already spans the whole sequence, so Windowed-MTP *degenerates to native MTP* at no cost: there is never a correctness reason to disable it, and a server can gate it on a context-length threshold. For the remaining knob W, at 1M and d=7 every window from 1K to 8K is net-positive on all three models (median 1.14–1.35×, Table 3), and each model's speedup varies by at most 0.06 across windows, so W needs no per-input tuning. We use W=4032, n_{sink}=64 everywhere.

Adaptive draft depth. Because windowing changes the context-dependent part of the draft cost from $\propto d \cdot S$ to $\propto d \cdot W$ (§3), the best draft depth is set mostly by acceptance rather than by a rising draft tax: the windowed optimum is d=7 on Qwen-35B but d=4 on the other two models (Table 5). An *adaptive-d* controller is therefore appealing and cheap under windowing, and we leave it to future work. Our headline numbers fix d=7 to contrast native and windowed at the *same* depth; windowing also wins on every model when each method uses its own best depth.

Composition, precision, and prefill. Three scope questions have short answers, developed in App. E. Windowing changes which KV the draft reads, not the shape of the candidate set, so it composes with tree speculation unchanged, needing only a wider ring ($n_{\text{sink}}+W+d\cdot k$ for width k). Under fp8 KV the per-step speedup narrows to 1.14–1.26× at 261K and 1M but persists, since windowing cuts the *number* of entries read while the dtype sets bytes per entry. Finally, prefill leaves a further gain untapped. During prefill the draft runs its layer over all S prompt tokens and writes a key/value entry for each, but once decoding starts the window reads only the sink and the last W of them; the rest are written once and never read. The draft could therefore skip those positions during prefill, turning its $O(S)$ draft prefill into an $O(W+n_{\text{sink}})$ one and cutting TTFT. Our gains are decode-side only, and that kernel work—the one lever that would also lift the prefill-bound ceiling of App. F—is future work.

Limitations. (1) The size of the gain depends on the draft and the framework. Windowing saves only the draft's attention read, so a draft whose step is dominated by other work gains less. All three MTP heads have 2 KV heads, but Nemotron's are half as wide (head_dim=128 vs. 256), so its draft reads half the KV bytes per token, and its MoE FFN is heavier (top-22 of 512 experts vs. top-8 of 256); its gain is 1.28× versus 1.30–1.44× for the Qwen drafts (Table 1). Part of the saving also comes from the draft's full-context KV-index build, which windowing removes along with the reads; an engine with a cheaper index build would see a smaller gain, but windowing would still be 1.07–1.16× faster per step even if that build cost nothing (App. B). (2) Headline numbers are B=1, TP1, single-GPU medians over 15–16 prompts per task, one run each. Acceptance in §5 pools all prompts; the cost (nearly constant across prompts), top-1 and attention-mass analyses use one. The advantage is not confined to B=1: a batch sweep to B=6 (Fig. 4), a TP2 sweep to B=12 (Fig. 5),

and a continuous-arrival run (App. F) all show windowing ahead. (3) Distribution preservation is exact only in exact arithmetic: `bf16` batched verification is not bit-exact against dense for either draft (§4).

8 Conclusion

Beside a hybrid target at 1M, a shipped full-attention MTP head's KV reads are a large share of the decode step and can make deep speculation slower than none. A training-free, serving-time window on draft attention (Windowed-MTP) removes most of that working set. At 1M it delivers a nearly input-invariant 1.28–1.44× acceptance-free per-decode-step speedup on three models from two hybrid families, and the gap grows with context. Acceptance falls on most tasks, by at most 19% per task, but the cheaper step outweighs it: at the default window the paired median favors windowing on every model–task cell at B=1. A ring buffer turns the smaller working set into physical capacity: 7.7–11.1% of total KV at 1M.

References

Yushi Bai, Shangqing Tu, Jiajie Zhang, Hao Peng, Xiaozhi Wang, Xin Lv, Shulin Cao, Jiazheng Xu, Lei Hou, Yuxiao Dong, Jie Tang, and Juanzi Li. LongBench v2: Towards deeper understanding and reasoning on realistic long-context multitasks. *arXiv preprint arXiv:2412.15204*, 2024.

Tianle Cai, Yuhong Li, Zhengyang Geng, Hongwu Peng, Jason D Lee, Deming Chen, and Tri Dao. Medusa: Simple LLM inference acceleration framework with multiple decoding heads. In *International Conference on Machine Learning (ICML)*, 2024.

Jungyoub Cha, Hyunjong Kim, and Sungzoon Cho. SpecExtend: A drop-in enhancement for speculative decoding of long sequences. In *Findings of the Association for Computational Linguistics (ACL Findings)*, 2026. arXiv:2505.20776.

Charlie Chen, Sebastian Borgeaud, Geoffrey Irving, Jean-Baptiste Lespiau, Laurent Sifre, and John Jumper. Accelerating large language model decoding with speculative sampling. *arXiv preprint arXiv:2302.01318*, 2023a.

Jian Chen, Yesheng Liang, and Zhijian Liu. DFlash: Block diffusion for flash speculative decoding, 2026. arXiv:2602.06036.

Shouyuan Chen, Sherman Wong, Liangjian Chen, and Yuandong Tian. Extending context window of large language models via positional interpolation. *arXiv preprint arXiv:2306.15595*, 2023b.

Tri Dao and Albert Gu. Transformers are SSMs: Generalized models and efficient algorithms through structured state space duality. In *International Conference on Machine Learning (ICML)*, 2024.

DeepSeek-AI. DeepSpec: A full-stack codebase for training and evaluating speculative decoding algorithms, 2026. `https://github.com/deepseek-ai/DeepSpec`.

DeepSeek-AI, Aixin Liu, Bei Feng, Bing Xue, Bingxuan Wang, Bochao Wu, Chengda Lu, Chenggang Zhao, Chengqi Deng, Chenyu Zhang, Chong Ruan, Damai Dai, Daya Guo, Dejian Yang, Deli Chen, Dongjie Ji, Erhang Li, Fangyun Lin, Fucong Dai, Fuli Luo, Guangbo Hao, Guanting Chen, Guowei Li, H. Zhang, Han Bao, Hanwei Xu, Haocheng Wang, Haowei Zhang, Honghui Ding, Huajian Xin, Huazuo Gao, Hui Li, Hui Qu, J. L. Cai, Jian Liang, Jianzhong Guo, Jiaqi Ni, Jiashi

Li, Jiawei Wang, Jin Chen, Jingchang Chen, Jingyang Yuan, Junjie Qiu, Junlong Li, Junxiao Song, Kai Dong, Kai Hu, Kaige Gao, Kang Guan, Kexin Huang, Kuai Yu, Lean Wang, Lecong Zhang, Lei Xu, Leyi Xia, Liang Zhao, Litong Wang, Liyue Zhang, Meng Li, Miaojun Wang, Mingchuan Zhang, Minghua Zhang, Minghui Tang, Mingming Li, Ning Tian, Panpan Huang, Peiyi Wang, Peng Zhang, Qiancheng Wang, Qihao Zhu, Qinyu Chen, Qiushi Du, R. J. Chen, R. L. Jin, Ruiqi Ge, Ruisong Zhang, Ruizhe Pan, Runji Wang, Runxin Xu, Ruoyu Zhang, Ruyi Chen, S. S. Li, Shanghao Lu, Shangyan Zhou, Shanhuang Chen, Shaoqing Wu, Shengfeng Ye, Shengfeng Ye, Shirong Ma, Shiyu Wang, Shuang Zhou, Shuiping Yu, Shunfeng Zhou, Shuting Pan, T. Wang, Tao Yun, Tian Pei, Tianyu Sun, W. L. Xiao, Wangding Zeng, Wanjia Zhao, Wei An, Wen Liu, Wenfeng Liang, Wenjun Gao, Wenqin Yu, Wentao Zhang, X. Q. Li, Xiangyue Jin, Xianzu Wang, Xiao Bi, Xiaodong Liu, Xiaohan Wang, Xiaojin Shen, Xiaokang Chen, Xiaokang Zhang, Xiaosha Chen, Xiaotao Nie, Xiaowen Sun, Xiaoxiang Wang, Xin Cheng, Xin Liu, Xin Xie, Xingchao Liu, Xingkai Yu, Xinnan Song, Xinxia Shan, Xinyi Zhou, Xinyu Yang, Xinyuan Li, Xuecheng Su, Xuheng Lin, Y. K. Li, Y. Q. Wang, Y. X. Wei, Y. X. Zhu, Yang Zhang, Yanhong Xu, Yanhong Xu, Yanping Huang, Yao Li, Yao Zhao, Yaofeng Sun, Yaohui Li, Yaohui Wang, Yi Yu, Yi Zheng, Yichao Zhang, Yifan Shi, Yiliang Xiong, Ying He, Ying Tang, Yishi Piao, Yisong Wang, Yixuan Tan, Yiyang Ma, Yiyuan Liu, Yongqiang Guo, Yu Wu, Yuan Ou, Yuchen Zhu, Yuduan Wang, Yue Gong, Yuheng Zou, Yujia He, Yukun Zha, Yunfan Xiong, Yunxian Ma, Yuting Yan, Yuxiang Luo, Yuxiang You, Yuxuan Liu, Yuyang Zhou, Z. F. Wu, Z. Z. Ren, Zehui Ren, Zhangli Sha, Zhe Fu, Zhean Xu, Zhen Huang, Zhen Zhang, Zhenda Xie, Zhengyan Zhang, Zhewen Hao, Zhibin Gou, Zhicheng Ma, Zhigang Yan, Zhihong Shao, Zhipeng Xu, Zhiyu Wu, Zhongyu Zhang, Zhuoshu Li, Zihui Gu, Zijia Zhu, Zijun Liu, Zilin Li, Ziwei Xie, Ziyang Song, Ziyi Gao, and Zizheng Pan. DeepSeek-V3 technical report. *arXiv preprint arXiv:2412.19437*, 2024.

Doğaç Eldenk, Payal Mohapatra, Yigitcan Comlek, Kaan Oktay, Hongyang Zhang, and Stephen Xia. Attention drift: What autoregressive speculative decoding models learn. *arXiv preprint arXiv:2605.09992*, 2026.

Gemma Team, Sherif El Abd, Vaibhav Aggarwal, Robin Algayres, Alek Andreev, Olivier Bachem, Ian Ballantyne, Cormac Brick, Victor Cărbune, Michelle Casbon, Mayank Chaturvedi, Aditya Chawla, Victor Cotruta, Alice Coucke, Phil Culliton, Robert Dadashi, Lucas Dixon, Mohamed Elhawaty, Utku Evci, Clément Farabet, Johan Ferret, Filippo Galgani, Sertan Girgin, Jean-Bastien Grill, Maarten Grootendorst, Jiaxian Guo, Cassidy Hardin, Yanzhang He, Steven M. Hernandez, Omri Homburger, Léonard Hussenot, Juyeong Ji, Armand Joulin, Aishwarya Kamath, Parnian Kassraie, Olivier Lacombe, Preethi Lahoti, Gaël Liu, Gus Martins, Luciano Martins, Tatiana Matejovicova, Ramona Merhej, Nikola Momchev, Sneha Mondal, Ryan Mullins, Sindhu Raghuram Panyam, Shreya Pathak, Sarah Perrin, André Susano Pinto, Etienne Pot, Angéline Pouget, Alexandre Ramé, Sabela Ramos, Douglas Reid, David Rim, Morgane Rivière, Karsten Roth, Louis Rouillard, Omar Sanseviero, Pier Giuseppe Sessa, Shane Settle, Danila Sinopalnikov, Sara Smoot, Piotr Stanczyk, Andreas Steiner, Lawrence Stewart, Ilya Tolstikhin, Michael Tschannen, Anton Tsitsulin, Nino Vieillard, Renjie Wu, Pingmei Xu, Haichuan Yang, Edouard Yvinec, Biao Zhang, Li Zhang, Joe Zou, Nicolas Aagnes, Abdelrahman Abdelhamed, Jakub Adamek, Shivani Agrawal, Shubham Agrawal, Ibrahim Alabdulmohsin, Jean Baptiste Alayrac, Uri Alon, Chandramouli Amarnath, Ankesh Anand, Chrysovalantis Anastasiou, Setareh Ariafar, François-Xavier Aubet, Kyriakos Axiotis, Federico Barbero, Joelle Barral, Alexei Bendebury, Urs Bergmann, Stanley Bileschi, Kat Black, Mathieu Blondel, Sebastian Borgeaud, Arthur Bražinskas, Ryan Burnell, Robert Busa-Fekete, Mu Cai, Daniele Calandriello, Glenn Cameron, Charlotte Caucheteux, Rahma Chaabouni, Garima Chadha, Jetha Chan, Blake Jianhang Chen, Jesse Chen, Lin Chen, Xu Chen, Derek

Cheng, Tzu-hsiang Chien, Nikolai Chinaev, Yi Chou, Zhaohui Chu, Benjamin Coleman, Pooja Consul, Sam Conway-Rahman, Scott Crowell, Dylan Cutler, Vivek Dani, Samira Daruki, Anil Das, Daniel Deutsch, Nishanth Dikkala, Li Ding, Qiuhan Ding, Shenil Dodhia, Konstantin Donhauser, Tulsee Doshi, Anca Dragan, Alex Druinsky, Sahil Dua, Zoltan Egyed, Danielle Eisenbud, Daniel Eppens, Cindy Fan, Bahare Fatemi, Yassir Fathullah, Vlad Feinberg, Milen Ferev, Sebastian Flennerhag, Takumi Fujimoto, João Gabriel Oliveira, Isaac Galatzer-Levy, João Gante, Simon Geisler, Soham Ghosal, Antonious M. Girgis, Tamara von Glehn, Alec Go, Alhaad Gokhale, Alex Grills, Yiming Gu, Mayank Gupta, Pramod Gupta, Guru Guruganesh, Raia Hadsell, Hamza Harkous, Jitendra Harlalka, Demis Hassabis, Anja Hauth, Joe Heyward, Arian Hosseini, Chih-Yang Hsia, I-Hung Hsu, Xiaopeng Huang, Yangsibo Huang, Kevin Hui, Adrian Hutter, Te I, Fotis Iliopoulos, Advait Jain, Ganesh Jawahar, Ziwei Ji, Qilin Jin, Melvin Johnson, Kandarp Joshi, Arun Kandoor, Wang-Cheng Kang, Koray Kavukcuoglu, Mehran Kazemi, Kathleen Kenealy, Amr Khalifa, Phoebe Kirk, Ivan Korotkov, Suraj Kothawade, Vitaly Kovalev, Neel Kovelamudi, Adam Kraft, Ravin Kumar, Vivek Kumar, Harish Kuppam, Justin Lannin, Chen-Yu Lee, Seungji Lee, Dmitry Lepikhin, Alon Levkovitch, Dongdong Li, Qiujia Li, Valentin Liévin, Ethan Lin, Ziqian Lin, Casper Liu, Tianlin Liu, Tianqi Liu, Xin Liu, Ivan Lobov, Mayank Lunayach, Min Ma, Gagan Madan, Andrii Maksai, Eric Malmi, Michal Matuszak, Daniel McDuff, Gaurav Menghani, Maciej Mikuła, Daniil Mirylenka, Karolis Misiunas, Vedant Misra, Andreea Mitran, Kareem Mohamed, Maksim Mukha, Eric Noland, James O'Donnell, Brendan O'Donoghue, Kate Olszewska, Bernett Orlando, Wanqiong Pan, Rina Panigrahy, Unnati Parekh, Nicolas Perez-Nieves, Chunjong Park, Eric Paskie, Liqian Peng, Bryce Petrini, Slav Petrov, Jonas Pfeiffer, Bilal Piot, Martyna Plomecka, Siim Poder, Octavio Ponce, Arijit Pramanik, David Racz, Anish Rajan, Michelle Ramanovich, Anand Rao, Marvin Ritter, Vitor Rodrigues, Evan Rosen, Mikołaj Rybiński, Noveen Sachdeva, Michaël E. Sander, Rohit Sathyanarayana, Sagar Savla, Samuel Schmidgall, Tal Schuster, George Scrivener, Benoit Seguin, Andrew Sellergren, Aliaksei Severyn, Izhak Shafran, Dhruv Shah, Bobak Shahriari, Yuan Shangguan, Ashish Shenoy, Pradeep Shenoy, Rakesh Shivanna, Pauline Sho, Lucas Spangher, Wojciech Stokowiec, Tim Strother, Yao Su, Yinghao Sun, Mukund Sundararajan, Andrea Tacchetti, Mor Hazan Taege, Pouya Tafti, Jean Tarbouriech, Chetan Tekur, Shantanu Thakoor, Rahul Thapa, Madeleine Traverse, Lenart Treven, Tao Tu, Chien Te Tung, Çağlar Ünlü, Petar Veličković, Malini Pooni Venkat, Sagar Gubbi Venkatesh, Vidya Venkiteswaran, Francesco Visin, Alex Vitvitskyi, Kiran Vodrahalli, Weiyi Wang, Xin Wang, Tris Warkentin, Jan Wassenberg, John Wieting, Cindy Wu, Lechao Xiao, Hao Xu, Yuhui Xu, Fuzhao Xue, Arun Yadav, Jun Yan, Antoine Yang, Lin Yang, Ming-Hsuan Yang, Ziyu Ying, Jae Hyeon Yoo, Morteza Zadimoghaddam, Sajjad Zafar, Fred Zhang, Jiageng Zhang, Jianyi Zhang, Xiaofan Zhang, Chao Zhao, David Zhou, and Chen Zou. Gemma 4 technical report, 2026. arXiv preprint arXiv:2607.02770.

Albert Gu and Tri Dao. Mamba: Linear-time sequence modeling with selective state spaces. *arXiv preprint arXiv:2312.00752*, 2023.

Cheng-Ping Hsieh, Simeng Sun, Samuel Kriman, Shantanu Acharya, Dima Rekesh, Fei Jia, Yang Zhang, and Boris Ginsburg. RULER: What's the real context size of your long-context language models? In *Conference on Language Modeling (COLM)*, 2024.

Yuri Kuratov, Aydar Bulatov, Petr Anokhin, Ivan Rodkin, Dmitry Sorokin, Artyom Sorokin, and Mikhail Burtsev. BABILong: Testing the limits of LLMs with long context reasoning-in-a-haystack. *Advances in Neural Information Processing Systems (NeurIPS)*, 2024.

Woosuk Kwon, Zhuohan Li, Siyuan Zhuang, Ying Sheng, Lianmin Zheng, Cody Hao Yu, Joseph E

Gonzalez, Hao Zhang, and Ion Stoica. Efficient memory management for large language model serving with PagedAttention. *Symposium on Operating Systems Principles (SOSP)*, 2023.

Yaniv Leviathan, Matan Kalman, and Yossi Matias. Fast inference from transformers via speculative decoding. In *International Conference on Machine Learning (ICML)*, 2023.

Yuhui Li, Fangyun Wei, Chao Zhang, and Hongyang Zhang. EAGLE: Speculative sampling requires rethinking feature uncertainty. In *International Conference on Machine Learning (ICML)*, 2024a.

Yuhui Li, Fangyun Wei, Chao Zhang, and Hongyang Zhang. EAGLE-2: Faster inference of language models with dynamic draft trees. *arXiv preprint arXiv:2406.16858*, 2024b.

Yuhui Li, Fangyun Wei, Chao Zhang, and Hongyang Zhang. EAGLE-3: Scaling up inference acceleration of large language models via training-time test. In *Annual Conference on Neural Information Processing Systems (NeurIPS)*, 2025.

Bowen Peng, Jeffrey Quesnelle, Honglu Fan, and Enrico Shippole. YaRN: Efficient context window extension of large language models. *arXiv preprint arXiv:2309.00071*, 2023.

Qwen Team. Qwen3.5: Towards native multimodal agents, 2026a. Model card: `https://huggingface.co/Qwen/Qwen3.5-122B-A10B`.

Qwen Team. Qwen3.6-35B-A3B: Agentic coding power, now open to all, 2026b. Model card: `https://huggingface.co/Qwen/Qwen3.6-35B-A3B`.

Ranajoy Sadhukhan, Jian Chen, Zhuoming Chen, Vashisth Tiwari, Ruihang Lai, Jinyuan Shi, Ian En-Hsu Yen, Avner May, Tianqi Chen, and Beidi Chen. MagicDec: Breaking the latency-throughput tradeoff for long context generation with speculative decoding. *arXiv preprint arXiv:2408.11049*, 2024.

Jianlin Su, Murtadha Ahmed, Yu Lu, Shengfeng Pan, Wen Bo, and Yunfeng Liu. RoFormer: Enhanced transformer with rotary position embedding. *Neurocomputing*, 568, 2024.

Jiaming Tang, Yilong Zhao, Kan Zhu, Guangxuan Xiao, Baris Kasikci, and Song Han. Quest: Query-aware sparsity for efficient long-context LLM inference. In *International Conference on Machine Learning (ICML)*, 2024.

Thinking Machines Lab. Inkling, 2026. Model card, July 2026. `https://thinkingmachines.ai/model-card/inkling/`.

Guangxuan Xiao, Yuandong Tian, Beidi Chen, Song Han, and Mike Lewis. Efficient streaming language models with attention sinks. In *International Conference on Learning Representations (ICLR)*, 2024.

Xiaomi LLM-Core Team, Bangjun Xiao, Bingquan Xia, Bo Yang, Bofei Gao, Bowen Shen, Chen Zhang, Chenhong He, Chiheng Lou, Fuli Luo, Gang Wang, Gang Xie, Hailin Zhang, Hanglong Lv, Hanyu Li, Heyu Chen, Hongshen Xu, Houbin Zhang, Huaqiu Liu, Jiangshan Duo, Jianyu Wei, Jiebao Xiao, Jinhao Dong, Jun Shi, Junhao Hu, Kainan Bao, Kang Zhou, Lei Li, Liang Zhao, Linghao Zhang, Peidian Li, Qianli Chen, Shaohui Liu, Shihua Yu, Shijie Cao, Shimao Chen, Shouqiu Yu, Shuo Liu, Tianling Zhou, Weijiang Su, Weikun Wang, Wenhan Ma, Xiangwei Deng, Bohan Mao, Bowen Ye, Can Cai, Chenghua Wang, Chengxuan Zhu, Chong Ma, Chun Chen, Chunan Li, Dawei Zhu, Deshan Xiao, Dong Zhang, Duo Zhang, Fangyue Liu, Feiyu Yang,

Fengyuan Shi, Guoan Wang, Hao Tian, Hao Wu, Heng Qu, Hongfei Yi, Hongxu An, Hongyi Guan, Xing Zhang, Yifan Song, Yihan Yan, Yihao Zhao, Yingchun Lai, Yizhao Gao, Yu Cheng, Yuanyuan Tian, Yudong Wang, Zhen Tang, Zhengju Tang, Zhengtao Wen, Zhichao Song, Zhixian Zheng, Zihan Jiang, Jian Wen, Jiarui Sun, Jiawei Li, Jinlong Xue, Jun Xia, Kai Fang, Menghang Zhu, Nuo Chen, Qian Tu, Qihao Zhang, Qiying Wang, Rang Li, Rui Ma, Shaolei Zhang, Shengfan Wang, Shicheng Li, Shuhao Gu, Shuhuai Ren, Sirui Deng, Tao Guo, Tianyang Lu, Weiji Zhuang, Weikang Zhang, Weimin Xiong, Wenshan Huang, Wenyu Yang, Xin Zhang, Xing Yong, Xu Wang, Xueyang Xie, Yilin Jiang, Yixin Yang, Yongzhe He, Yu Tu, Yuanliang Dong, Yuchen Liu, Yue Ma, Yue Yu, Yuxing Xiang, Zhaojun Huang, Zhenru Lin, Zhipeng Xu, Zhiyang Chen, Zhonghua Deng, Zihan Zhang, and Zihao Yue. MiMo-V2-Flash technical report, 2026. arXiv preprint arXiv:2601.02780.

Penghui Yang, Cunxiao Du, Fengzhuo Zhang, Haonan Wang, Tianyu Pang, Chao Du, and Bo An. LongSpec: Long-context lossless speculative decoding with efficient drafting and verification. In *Proceedings of the 64th Annual Meeting of the Association for Computational Linguistics (Volume 1: Long Papers) (ACL)*, pages 1826–1844, 2026.

Lianmin Zheng, Liangsheng Yin, Zhiqiang Xie, Chuyue Sun, Jeff Huang, Cody Hao Yu, Shiyi Cao, Christos Kozyrakis, Ion Stoica, Joseph E. Gonzalez, Clark Barrett, and Ying Sheng. SGLang: Efficient execution of structured language model programs. *Advances in Neural Information Processing Systems (NeurIPS)*, 2024.

A Experimental details

How the 1M inputs are built. We never tile or repeat text. RULER inputs follow RULER's construction (needles and queries hidden in a distractor haystack of controlled length). LongBench-v2 and BABILong use real documents longer than 1M tokens, cut from the end to length. Every input comes from a seeded generator and is byte-identical across runs.

Models (exact checkpoints). `RedHatAI/Qwen3.6-35B-A3B-NVFP4` and `nvidia/Qwen3.5-122B-A10B-NVFP4` (NVFP4 weights, with a YaRN `rope_scaling` factor of 4 applied to the `config.json` to reach 1M from the native 262,144-token window) and `nvidia/NVIDIA-Nemotron-3-Super-120B-A12B-NVFP4` (NVFP4, native NoPE attention, so no RoPE change). All three have quantized weights. The checkpoints ship FP8 KV scales, which we override so that every run stores KV in bf16 (`kv_cache_dtype=bfloat16`).

Engine and flags. We serve with SGLang 0.5.12.post1 (commit `3489ce04`) plus our patch (Windowed-MTP and the draft-KV ring buffer; `https://github.com/avalliappan-nvidia/windowed-mtp-b200/tree/master`). The windowing is merged upstream as SGLang PR #32673 (`--speculative-draft-window-size`, `--speculative-draft-sink-size`); the ring buffer is not yet upstream. All B200 and H100 runs use one image (NGC `sglang:26.06-py3`: FlashInfer 0.6.12, Triton 3.6.0, PyTorch 2.13.0a0, CUDA 13.3). `mem-fraction-static` is 0.85 for single-request runs. In the batch and Pareto sweeps each arm uses the highest value at which it starts and serves the batch (0.87–0.98). The fraction reserves memory for the weights and the target KV pool; CUDA-graph capture, activations and the draft worker's buffers must fit in the rest. Native's draft worker must also allocate a full-length draft KV pool, so native reaches its limit at a lower fraction; with the prefix cache on, it fails to start at 0.90 while allocating that pool, a single 6.25 GiB buffer

(App. F). The windowed pool holds only $n_{\text{sink}}+W+d$ slots per request, so the windowed arm can give more memory to the target KV. The frontier therefore compares each arm's best feasible serving configuration, not equal fractions. On Qwen-122B (0.90) and Nemotron (0.87) every arm uses the same fraction.

Why the extra Qwen-35B request is a fair comparison. Both arms run on the same GPU with the same weights and start from the same 177.6 GiB of free memory; the memory fraction only sets how SGLang splits it. The difference is the draft KV pool. Native's draft pool stores every token of the target pool. At its highest working fraction, 0.92, the target pool holds 5.77M tokens, the draft pool takes 11.0 GiB, and 3.1 GiB is left. A sixth 1M request needs a ≈6.24M-token pool. Each extra token costs native 22 KiB: 20 KiB of target KV (10 full-attention layers × 2 KV heads × 256 dims × K and V in bf16) plus 2 KiB of draft KV (one layer). It would need ≈9.9 GiB more, over three times what is left. A higher fraction does not help: at 0.98 native fails to start, because its draft pool must fit in the 2% outside the fraction. The ring needs only 4,103 draft slots (8 MiB) per request; its pool reserves them for SGLang's 39 maximum running requests (160,017 slots, 0.3 GiB in all). The windowed arm therefore runs at 0.98 with a 6.28M-token pool, seats six, and still has 1.9 GiB free after allocating its draft pool. The speedup does not depend on that extra memory: with windowing at 0.90 (5.60M tokens), below native's 0.92, both arms seat five and queue the sixth, and windowing is still 1.21× faster per token at B=5 (9.83 vs. 11.89 ms). The sixth request is therefore what the ring's freed draft memory buys on the same GPU.

Other settings: `page-size 1`, FlashInfer target attention, CUDA graphs on, and MTP speculation (SGLang's `NEXTN` algorithm) with `num-steps`= $\gamma = d-1$ and `eagle-topk 1`. All generation arms use repetition penalty 1.15; without it, long greedy enumeration answers can fall into repetition loops, which are easy to predict and inflate acceptance. Native MTP uses the FlashInfer draft backend; Windowed-MTP uses the Triton draft backend, where we implemented the ring remap, with W=4032 and n_{sink}=64.

Measurement protocol. Every input is 1,040,000 tokens. Each run does one tiny warmup generation, flushes the cache, then a timed prefill and decode. TPOT comes from SGLang's per-step log (`decode-log-interval 1`). Line i reports the batch-mean accept length AL_i and the aggregate throughput X_i over that step, so the step's wall time is $\Delta t_i = B_{\text{eff}}\text{AL}_i/X_i$. Over steady steps (those at the full batch B_{eff} after a two-step ramp, clipped to 0.4–2.5× the median Δt_i) we set $\text{TPOT} = \text{med}_i(\Delta t_i)/\overline{\text{AL}}$, with $\overline{\text{AL}}$ taken over the same steps. At B=1 this matches the direct estimate $B_{\text{eff}}\sum_i \Delta t_i/\sum_i N_i$ ($N_i = B_{\text{eff}}\text{AL}_i$ committed tokens) over all steady steps to within 0.6% on every cell of the single-prompt sweep, and the clip removes no steps. For B>1 sweeps (Figs. 4 and 5) we use that direct estimate, unclipped, over the first full-batch stretch: from the first step at full concurrency (after the ramp) to the first request finishing or being admitted. Later steps mix KV teardown and re-admission prefill into the step log. The stretch keeps a one-time ∼200 ms stall that speculative runs show early in decode; on short Nemotron decodes it adds up to ∼30% to TPOT.

Fixed-batch runs use real-input QA, stopping at EOS or 512 tokens. Batch and Pareto sweeps (Figs. 4 and 5) copy one record across the batch with the radix cache off, so each request holds its own full 1M KV. The online run is the exception (App. F).

Statistical protocol. Each cell of Table 4 runs 16 prompts per task (records 0–15 of the seeded generator; Code-QA has 15), one seeded run each, and reports the median over prompts; the dense baseline runs the same prompts. Table 16 gives 95% bootstrap intervals (10^4 resamples) for the

median AL ratio and the median nat/win. Nemotron answers NIAH-s, VT, Code-QA and BABILong in 4–12 tokens (1–2 verify steps), which leaves no steady decode to time, so those cells are omitted. Within one run, TPOT is a median over the steady steps, and a repeated greedy run reproduces it within about 1%. Fig. 2 pools the acceptance histograms of these same runs over all prompts and inputs. Decode steps within one prompt are correlated, so its 95% intervals come from a cluster bootstrap over prompts, stratified by input. Unless stated otherwise, the other fixed-batch analyses use one prompt (record 0, the first of the 16).

The windowing change (pseudocode). Windowed-MTP changes only a few lines in the code that builds the draft's per-request KV index. The target verification path is untouched.

```
# draft step, req r, seq len S:
if WINDOW and S > n_sink + W:
    keep = range(0, n_sink)   # sink
         + range(S - W, S)    # window
else:
    keep = range(0, S)        # short
kv_index = req_to_token[r, keep]
# RING: slot = ring_base(r) + logical_pos
#       modulus = n_sink + W + d
```

RoPE is already applied to the cached keys, so shrinking the index does not change any key's position. No new kernel or attention mask is needed, and the path is CUDA-graph safe.

The ring buffer. With the ring on, the draft's KV pool holds $n_{\text{sink}}{+}W{+}d$ slots per request instead of one slot per token. With $s{=}n_{\text{sink}}$ and $M{=}W{+}d$, a token at position p of request r is stored at a slot that depends only on (r, p):

$$\text{slot}(r,p) = r\,(s{+}M) + \begin{cases} p, & p < s, \\ s + (p-s) \bmod M, & p \geq s. \end{cases}$$

The sink positions are written once; the rest wrap around a band of $W{+}d$ slots. A draft step reads the sink plus the last W positions and writes at most d new ones, a span of at most $W{+}d$ consecutive positions, so all map to distinct slots and the draft never reads an overwritten entry. Rejection needs no rollback: beyond the committed sequence, the draft reads only positions written in the current step, and a rejected token's slot is overwritten when the committed token is written there. The target's KV, allocator and position map are unchanged. The patch requires the Triton draft backend and refuses tree drafts (`eagle-topk`>1) with page size above one.

B Latency-model fit

Acceptance-free per-iteration time. We fit time per iteration rather than TPOT, so acceptance does not enter. The scheduler reports each iteration's accepted tokens AL_i and throughput X_i, so its wall time is $T_{\text{iter},i} = \text{AL}_i / X_i = \text{AL}_i \cdot \text{TPOT}_i$, in which AL cancels. It depends on the hardware and context length, not on the workload.

The fit. Following Eq. 1, $T_{\text{iter}}(\gamma) = c + \gamma\, t_{\text{draft}}^{\text{fwd}}$ with $c \equiv t_{\text{verify}} + t_{\text{draft}}^{\text{ctx}}$. We sweep γ and fit this line by least squares over $\gamma \in [4, 7]$ ($d{=}5$–8; Qwen-122B over $\gamma \in [4, 6]$, since $d{=}8$ does not fit at 1M), after the one-time verify jump at $d{=}5$ explained below. On `niah_multiquery_enum` (Table 1) the fit is tight ($R^2{\geq}0.97$ for both arms), and windowing lowers both terms.

The intercept falls by $\Delta c \approx 5.1$–6.1 ms. Windowing leaves t_{verify} unchanged on the Qwen models, so this is mostly the draft's index build. Two kernels build that index over the whole context, `generate_draft_decode_kv_indices` (≈3.5 ms per iteration) and `create_flashinfer_kv_indices` (≈1 ms), and both drop to nearly zero under windowing (Table 8). This saving depends on the implementation. The slope falls by 0.3–0.5 ms per forward (≈1.9–2.9 ms at γ=6); it comes from each forward reading a bounded window, so it holds on any backend.

If native's index build cost nothing. To bound how much a leaner index would erase, we give native the whole intercept drop for free: $(\text{step}^{\text{nat}} - |\Delta c|)/\text{step}^{\text{win}}$. This is native's best case: a bandwidth-bound build of the ≈4 MB index of a 1M request takes a few microseconds, and Δc also contains Nemotron's 1.2 ms bookkeeping drop, which is not index work. Windowing still wins per step: 1.16× on Qwen-35B (21.3 vs. 18.3 ms), 1.07× on Qwen-122B (28.4 vs. 26.5) and 1.07× on Nemotron (27.6 vs. 25.8; 1.12× if the bookkeeping drop is kept). What remains is the per-forward read saving.

The verify jump at d=5. In a finer sweep over γ (to γ=6 on Qwen-122B and 7 on Nemotron, the deepest that fit a 1M request), native T_{iter} on Qwen-122B and Nemotron jumps between γ=3 and 4 (24.8→32.2 and 24.5→30.7 ms). An nsys profile places ≈90% of it in the verify attention: going from 4 to 5 query rows pushes FlashInfer's paged-prefill kernel past a tile boundary, roughly doubling its cost per call (593→1133 μs). This adds ≈6 ms once to t_{verify}, and so to c. It leaves the slope unchanged and affects both arms equally, so it cancels in Δc. Fitting only after the jump keeps every point, including d=7, on the same side of it.

Table 8 lists the largest kernels in t_{draft} from the nsys trace behind Table 2. These are GPU-busy times, which exclude idle and CPU time and so sum to less than t_{draft}.

Table 8: Largest components of t_{draft} (nsys GPU-busy, d=7, 1M, B=1, μs/iter). The full-context index kernels collapse under windowing. Qwen-122B's slower windowed draft-extend is Triton's ragged extend kernel, not the window (App. E).

draft kernel (μs/iter)	q35	q122	nem
native (FlashInfer draft, full pool)			
`generate_draft_decode_kv_indices`	3588	3655	2891
`create_flashinfer_kv_indices` (draft)	1047	1068	1032
draft-decode attn (×6)	1608	1598	853
draft-extend attn	423	818	404
windowed+ring (Triton draft, compact pool)			
`generate_draft_decode_kv_indices`	3.0	3.1	3.1
ring index kernel	2.0	2.2	2.0
draft-decode attn (×6)	348	976	149
draft-extend attn	550	2908	143

C Predicting when native speculation loses

§6 shows that native speculation can be slower than none. The break-even AL of Eq. 2 uses only acceptance-free step times, so a server can compute it before any request arrives. Here we calibrate it on one input and check its calls on the rest.

The test. For each input we divide native's d=7 step time, measured on `niah_multiquery_enum` only (Table 1), by that input's dense TPOT to get its break-even AL, and flag native as losing when its measured AL falls below it (Table 9). 17 of the 20 cells are held out.

Table 9: Break-even check at d=7, 1M, B=1. Break-even AL is native's step time on `niah_multiquery_enum` (†; Table 1) over each input's dense TPOT; AL and dense are from Table 4. *inverts*: native slower than dense, predicted (p: AL below break-even) vs. measured (m). **Bold**: the three false positives; there are no misses.

model	input	AL	break-even	inverts (p/m)
q35	NIAH-s	5.07	2.68	– / –
	NIAH-mv	5.42	2.68	– / –
	NIAH-mq†	4.45	2.70	– / –
	VT	4.18	2.72	– / –
	CWE	2.74	2.87	**inv** / –
	FWE	2.85	2.86	**inv** / –
	Code-QA	3.30	2.65	– / –
	BABILong	3.07	2.74	– / –
q122	NIAH-s	4.04	3.62	– / –
	NIAH-mv	4.81	3.62	– / –
	NIAH-mq†	4.76	3.61	– / –
	VT	3.82	3.59	– / –
	CWE	3.28	3.89	inv / inv
	FWE	3.45	3.93	inv / inv
	Code-QA	3.16	3.60	inv / inv
	BABILong	3.64	3.70	**inv** / –
nem	NIAH-mv	2.86	2.92	inv / inv
	NIAH-mq†	3.63	2.91	– / –
	CWE	1.64	3.04	inv / inv
	FWE	1.64	3.03	inv / inv

Accuracy. All 6 cells where native is slower than dense are flagged, and the 3 false positives are near-ties: q35 CWE and FWE (native 1.05× and 1.07× dense) and q122 BABILong (1.00×, a tie). This is the less costly error: a server would turn speculation down slightly early rather than keep a losing configuration. The question only arises for native speculation: windowing's per-step saving does not depend on acceptance, and Windowed-MTP is ahead of native on every cell.

Where the error comes from. The calls assume step time is the same on every input. It nearly is: on 13 of the 20 cells native's median step is within 3% of the calibration value. The exceptions are the aggregation inputs (CWE and FWE), whose step is 7–9% shorter, likely because the draft-extend step scales with accepted tokens, and q35 BABILong (3.1%). A shorter step lowers the true break-even, so these inputs are flagged slightly early; the two q35 false positives come from this, and no call is missed.

Other depths. With native's step predicted by the line of Table 1 instead of measured, the test on the other inputs' single-prompt depth sweeps flags all 20 of 53 cells at d=5–8 where native loses (4 near-tie false positives, 1.00–1.06×). The line does not carry past a tile-boundary jump (d=2→3 on all models, d=9 on Qwen-35B), where a separate fit is needed.

D Per-position and decision-invariance details

Table 10 gives the numbers behind Fig. 2, pooled over all prompts and inputs. On the Qwen models native and windowed differ by at most 0.04 at any position (Qwen-122B at j=2, 0.78→0.74; Qwen-35B at j=3, 0.77→0.73), and α_1 by at most 0.02. Nemotron's windowed draft accepts more at every position. Deep positions have the fewest samples, most visibly on Nemotron, where about 200 steps per draft reach j=6. Single inputs vary more: the largest per-input change on Qwen is −0.18 (Qwen-35B NIAH-mv, j=2).

Table 10: Conditional acceptance α_j by draft position (d=7, 1M), pooled over all prompts and inputs of Table 4; the numbers behind Fig. 2.

model	draft	α_1	α_2	α_3	α_4	α_5	α_6
q35	native	0.77	0.75	0.77	0.77	0.77	0.79
	window	0.76	0.73	0.73	0.74	0.80	0.79
q122	native	0.80	0.78	0.75	0.78	0.81	0.81
	window	0.78	0.74	0.75	0.78	0.81	0.80
nem	native	0.45	0.52	0.63	0.38	0.38	0.20
	window	0.52	0.56	0.66	0.43	0.42	0.40

Direct decision-invariance probe. Acceptance depends on whether windowing changes the draft's *choice* of token. In the native run (1M, d=7, `niah_multiquery_enum`), at each decode step we rerun the draft head with the same hidden state, position and seed but with its KV cut to the sink and window, and compare the two top-1 proposals. Over 275–512 draft-head forwards (each speculative step runs several; the probe fires on every draft decode forward past 4K tokens of context and stops at 512 or when the standard 512-token generation ends, Table 11) the top-1 is unchanged 86–94% of the time. For Qwen-35B and Nemotron the flips fall at near-ties, where the full model's top-two logit gap is ≈0.5, against 3–5 on average. The size of the internal change does not decide this: under windowing Nemotron picks about half of its MoE experts differently (router-overlap Jaccard ≈0.5), yet keeps its top-1 86% of the time.

Qwen-122B is the exception. Its flips fall at confident positions (gap 6.8 against an average of 7.2): this strongest drafter uses distant context to tell needles apart, which explains its acceptance loss on this input (5.57→4.74 on the probed prompt; median ratio 0.89 over 16 prompts, Table 16). The target verifies every token, so this costs latency, never correctness. The probe is per step; whole-generation effects are measured by the windowed runs in Table 4.

Table 11: Decision-invariance probe (native draft, in-run A/B, eager; 1M, B=1, d=7, `niah_multiquery_enum`). *probes*: draft-head decode forwards compared, within the run's 512-token generation. *agree*: fraction of probes whose windowed top-1 equals the full-context top-1. *margin*: the full model's top-1/top-2 logit gap, over all steps and over flipped steps only.

model	probes	agree	flip	margin (all)	margin (flips)
q35	512	0.94	0.06	5.16	0.49
q122	465	0.87	0.13	7.18	6.80
nem	275	0.86	0.14	3.02	0.54

Why the decision holds. Both draft families sit on recurrent-hybrid models (Gated-DeltaNet for Qwen, Mamba2 for Nemotron, each with a few full-context GQA layers). Their recurrent layers already carry long-range information, so the draft's distant reread mostly repeats what it has, consistent with concurrent attention-drift findings (§2). How far the attention reaches depends on positional encoding (Table 12). The Qwen heads (length-extended RoPE) put ≈75–80% of their softmax mass inside the window, and windowing changes their attention output by ∼15%. The Nemotron head (NoPE) puts only ≈16% inside and its output changes by over 100%, yet its top-1 is equally preserved: the Mamba2 state already encodes that context, and the attention output's L2 norm is about half that of the hidden state it is added to ($\|W_o o\|/\|h_t\| \approx 0.5$). The size of the change therefore does not predict the token choice (Table 11).

Table 12: Attention mass of the native draft at the operating window (W=4032, sink 64; 1M, B=1, d=5, `niah_multiquery_enum`). in-win mass: softmax mass inside the window; win_perturb: relative L_2 change of the read-out $o = \sum_j p_j v_j$ when the far tail is dropped; tail out-frac: share of $\|o\|$ from far keys.

model	in-win mass	win_perturb	tail out-frac
q35	0.748	0.139	0.246
q122	0.805	0.169	0.184
nem	0.160	1.059	0.822

Windowing could lose acceptance where distant attention is *concentrated* on a few tokens that matter. The largest loss on this prompt is 15% (Qwen-122B), and across all tasks the largest task-level median loss is 19% (Qwen-35B NIAH-mv, not probed this way); the cost saving outweighs it on every cell. This is interpretation, not proof. Swapping the distant content in a controlled way would separate two explanations, distant attention diluting the prediction and length-extended RoPE degrading at long range; we leave that to future work.

E Ablations and scope notes

The backend is not the confound. Native MTP runs on FlashInfer, but we implemented the ring on the Triton draft backend, so the gain could in principle come from the backend. It does not: Triton is a handicap. At a matched point (Table 13), moving native to Triton makes its full-context draft-extend much slower, yet Windowed-MTP on Triton still beats native on FlashInfer. One caveat: Triton's ragged draft-extend grows with accept length, unlike FlashInfer's padded `BatchPrefill`, which can eat into the gain at high acceptance (Table 8). We have not built a FlashInfer ring, so its performance remains unmeasured.

Table 13: Backend ablation at a matched point (q35, d=5, 1M, CWE, B=1). Native on Triton is a deliberate stress test, not an operating point: Triton makes native's TPOT ∼6× worse, yet windowed on Triton beats native on FlashInfer.

draft path	backend	TPOT (ms)
native	FlashInfer	8.13
native	Triton	50.59
Windowed-MTP (ring buffer)	Triton	**5.37**

Robustness to KV-cache quantization. Windowing cuts the *number* of KV entries the draft reads (about 99% fewer at 1M); the KV dtype sets the bytes per entry. Under fp8 the draft still skips ≈99% of its KV bytes, but the absolute time saved scales with bytes per entry, so lower-precision KV shrinks the relative gain to the extent decode is KV-bandwidth bound. A sweep on `niah_multiquery_enum` confirms this (per-step ratio $\text{step}^{\text{nat}}/\text{step}^{\text{win}}$, in which acceptance cancels):

	261K		1M	
model	bf16	fp8	bf16	fp8
Qwen-35B	1.28×	1.20×	1.46×	1.22×
Qwen-122B	1.23×	1.14×	1.29×	1.15×
Nemotron	1.18×	1.16×	1.26×	1.26×

Windowing wins every cell (1.14–1.26× under fp8). This is a separate run, so its bf16 column differs slightly from Table 1. fp8 shrinks the Qwen gains (at 1M, 1.46→1.22× and 1.29→1.15×), while Nemotron, which reads less KV per token, is unchanged (1.26×). Verification still preserves the output distribution, and the reclaimable fraction of the draft pool is unchanged; only its size in GB scales. Our main numbers fix KV storage to bf16 for a controlled comparison and evaluate fp8 KV separately; our stack's fp8 KV path also lacks a fused attention kernel, which inflates absolute fp8 latency.

Compatibility with tree speculation. We evaluate chain speculation (`eagle-topk`=1). Windowing changes only which KV the draft reads, not the candidate tree, so it applies to tree speculation unchanged; only the ring grows, to $n_{\text{sink}}+W+d\cdot k$ slots for width k, still far below a full-length draft pool. Measuring it is future work.

Pruning the draft's prefill to lower TTFT. The draft builds its own KV over the prompt, one pass per prefill chunk, but under windowing it only reads the sink and the last W tokens. Skipping the intermediate chunks would shrink draft prefill from $O(S)$ to $O(W+n_{\text{sink}})$, removing almost all of it at 1M and lowering TTFT without touching the target or the output distribution. The kernel work is future work.

F Online serving under continuous arrivals

Workload. Qwen-35B at TP2 under SGLang's continuous-batching scheduler with the prefix cache on. Requests arrive as a Poisson process at rate λ (req/s), with input lengths of 131K, 262K, 524K and 1.04M tokens in a 4:3:2:1 ratio, drawn from the RULER QA corpora (`niah_multiquery_enum`, `cwe`, `fwe_enum`). Half of the requests ask a new question about an already-served context (measured prefix hit rate 0.69). We discard 8 warmup requests and report the next 32.

Controls. (1) One seed fixes the whole trace, so request i is the same work in every arm and requests can be compared in pairs. (2) With `ignore_eos` every request generates exactly 4096 tokens: at the main runs' 512-token cap decode is only 20–27% of request time next to a 1M prefill, against 45–74% at 4096. (3) All arms use `mem-fraction-static` 0.85; at 0.90 native fails to start while allocating its full-length draft pool (a single 6.25 GiB buffer), while dense and windowed run.

Results. Windowing's paired median speedup is 1.15–1.21× over native and 2.0–2.2× over dense (Table 14); the mean gain is larger (1.2–1.8×), so it is concentrated in long requests. Under a 25 ms

p95-TPOT SLO on the longest bucket, windowing sustains 0.05 req/s and both baselines only 0.02 (Table 15); windowing's worst bucket (22.8 ms) is below native's best (36.0 ms). With two rates and four 1.04M requests, this is a separation, not a capacity estimate. Online AL is 3.61–3.77 for native and 3.15–3.42 for windowed: windowing wins on cheaper steps, not on acceptance.

Table 14: Paired per-request decode latency, online trace (Qwen-35B TP2, 32 steady-state requests). wins: requests on which windowing is strictly faster.

	mean ms/token			paired median (wins)	
λ	dense	native	win	vs. dense	vs. native
0.02	9.92	6.50	**5.34**	2.02× (29/32)	1.15× (26/32)
0.05	26.26	18.87	**10.51**	2.23× (32/32)	1.21× (28/32)

Table 15: Per-bucket p95 TPOT (ms) at λ=0.05 and the highest tested rate (0.02 or 0.05) sustained under each SLO. Buckets are small (n=4 at 1.04M).

	p95 TPOT (ms) by input length				max sustained λ	
arm	131K	262K	524K	1.04M	25 ms	50 ms
dense	39.3	41.0	43.6	39.0	0.02	0.05
native	38.4	38.8	41.3	36.0	0.02	0.05
windowed	**18.2**	**21.2**	**12.1**	**22.8**	**0.05**	0.05

The ceiling is set by prefill. From 0.075 to 0.15 req/s offered, no arm keeps up: served rates level off at 0.054–0.063 req/s and p95 TTFT grows from 155 to 326 s. Windowing raises the rate a server can handle under a decode SLO, not peak throughput, which needs prefill work such as the draft-prefill pruning of App. E.

G Variation across prompts

Table 16 gives the per-prompt spread for every cell of Table 4. Native is faster on 18 of 318 prompts, and no cell's median favors native. The per-step speedup is nearly constant across prompts (cell medians within 3% of Table 1), so the spread in end-to-end speedup comes from acceptance.

Table 16: Per-prompt spread (d=7, 1M, B=1): medians of $\mathrm{AL}^{\mathrm{win}}/\mathrm{AL}^{\mathrm{nat}}$ and nat/win TPOT, 95% bootstrap CIs (10^4 resamples); range: min–max nat/win; nat faster: prompts with nat/win < 1.

model	input	n	AL ratio [95% CI]	nat/win [95% CI]	range	nat faster
q35	NIAH-s	16	0.94 [0.90, 0.98]	1.35 [1.30, 1.39]	1.21–1.46	0
	NIAH-mv	16	0.81 [0.75, 0.86]	1.15 [1.05, 1.17]	0.97–1.29	1
	NIAH-mq	16	0.96 [0.92, 1.02]	1.34 [1.29, 1.43]	1.19–1.63	0
	VT	16	0.84 [0.81, 0.98]	1.21 [1.16, 1.41]	1.05–1.71	0
	CWE	16	1.04 [0.96, 1.10]	1.45 [1.35, 1.53]	0.60–2.07	1
	FWE	16	1.11 [1.01, 1.28]	1.56 [1.45, 1.83]	1.26–2.34	0
	Code-QA	15	0.95 [0.90, 1.03]	1.37 [1.30, 1.50]	1.12–1.73	0
	BABILong	16	0.90 [0.85, 1.03]	1.28 [1.19, 1.43]	0.69–2.25	3
q122	NIAH-s	16	0.93 [0.91, 0.99]	1.21 [1.18, 1.28]	0.96–1.43	1
	NIAH-mv	16	0.87 [0.82, 0.92]	1.14 [1.06, 1.22]	1.00–1.45	2
	NIAH-mq	16	0.89 [0.86, 0.94]	1.16 [1.11, 1.23]	0.96–1.66	1
	VT	16	0.96 [0.89, 1.08]	1.25 [1.16, 1.40]	1.08–1.81	0
	CWE	16	0.98 [0.93, 1.09]	1.27 [1.20, 1.42]	1.14–1.65	0
	FWE	16	1.04 [0.98, 1.09]	1.34 [1.25, 1.39]	1.11–1.86	0
	Code-QA	15	1.01 [0.93, 1.05]	1.31 [1.23, 1.41]	0.97–1.67	1
	BABILong	16	0.90 [0.76, 0.96]	1.14 [0.98, 1.25]	0.70–1.73	4
nem	NIAH-mv	16	0.97 [0.93, 1.00]	1.26 [1.19, 1.30]	1.08–1.91	0
	NIAH-mq	16	1.00 [0.94, 1.07]	1.27 [1.20, 1.36]	0.66–3.19	1
	CWE	16	1.15 [1.04, 1.51]	1.47 [1.33, 1.97]	1.09–2.25	0
	FWE	16	1.19 [0.92, 1.49]	1.53 [1.19, 1.97]	0.71–3.31	3